Surface and interface properties for the Cu/W(110) system and their effect on oxygen adsorption

J. E. Houston, Peter J. Feibelman, and D. G. O'Neill*
Sandia National Laboratory, Albuquerque, New Mexico 87185

D. R. Hamann
AT&T Bell Laboratory, Murray Hill, New Jersey 07974
(Received 22 May 1991)

The results of angle-resolved ultraviolet photoemission measurements and electronic-structure calculations are presented for Cu adsorbed on the W(110) surface. Data as a function of Cu coverage suggest the existence of sets of surface and interface states resulting from the Cu-W interaction. Calculations corroborate this suggestion and identify the surface and interface character and orbital symmetries of the states. Near the zone boundary along the $\bar{\Gamma}$-$\bar{H}$ symmetry line, these states lie in gaps in the projected bulk band structure for the W(110) surface and are localized either within the Cu overlayer (surface states) or shared between the Cu and first W layer (interface states). Reasonable agreement is obtained between experiment and theory. We also performed low-energy electron diffraction and measured the behavior of the surface and interface states with O_2 coverage. We conclude that the enhancement of the O_2 dissociative sticking coefficient for the 1-monolayer Cu film results from an increase in the precursor-state accommodation coupled with the ability of Cu to displace easily giving O_2 continued access to the more active W surface.

I. INTRODUCTION

The unique chemical behavior associated with a metal monolayer (ML) adsorbed on the surface of a different metal has attracted considerable recent attention from the surface science community.[1] Nevertheless, few examples exist where this unique behavior has been directly related to the fundamental structural, electronic, or mechanical properties of the bimetallic surface. Consider the recent series of papers by Gomer and co-workers concerning the interaction of O_2 with the Cu/W(110) bimetallic system.[2-4] These authors find that the precursor-mediated dissociative sticking coefficient for low-coverage O_2 has values of approximately 0.5 for the clean surface, 1.0 for 1 ML Cu/W(110), and 0.5 for the second Cu ML. Further reductions are found for thicker Cu overlayers, and the clean Cu(111) value has been measured to be about 10^{-3}.[5]

To understand the origin of the unusual behavior of the 1-ML case, Gomer *et al.* both investigated its electronic properties by angle-integrated uv photoemission and analyzed the competition between the Cu and W for O bonding.[2-4] Although subtle differences are noted between the 1- and 2-ML photoemission results, these authors find no obvious source of the unit-sticking coefficient for 1 ML Cu.

Close inspection of the Cu-coverage dependence of the photoemission data of Gomer *et al.*[3] reveals evidence for the formation of interface states similar to those reported for growth of Cu and Ni on Ru(0001).[6,7] In order to explore whether these states might be responsible for the unique 1 ML Cu/W(110) O_2 chemistry, we report here the results of a detailed study of the electronic properties of the Cu/W(110) bimetallic system. We identify the states that show the angle-resolved ultraviolet photoemission (ARUPS) fingerprint for surface and interface-state behavior, map their dispersion along a selected symmetry line in the surface Brillouin zone (SBZ), and compare the results to surface electronic-structure calculations using the linearized augmented-plane-wave (LAPW) method. We find several localized Cu-W interface states and Cu surface states in the region near the zone boundary at $\bar{H}$. Agreement between experiment and theory is demonstrated, which allows the degree of surface or interface localization and the orbital makeup of these states to be identified.

We probe the possible role of the surface and interface states in O_2 dissociation by observing the changes in these states as O_2 is chemisorbed. We find that all surface-localized states are rapidly "poisoned" by adsorbed O. In other words, the surface states decrease in amplitude while the bonding-antibonding combination of interface states decreases in amplitude and then separates, moving the antibonding component toward the Fermi level. Using LEED, we find that O chemisorption results in some surface rearrangement as indicated by the appearance of outboard satellites along the $[1\bar{1}0]$ direction. We suggest that the unique increase in the O_2 dissociative sticking coefficient observed for the 1 ML Cu/W(110) system[3] results from better energy transfer from the O_2 to the lighter Cu surface atoms coupled with the ability of the Cu atoms to displace. This displacement allows O_2 continued access to the more active W surface.

II. EXPERIMENTAL AND THEORETICAL TECHNIQUES

A. Experimental techniques

The W(110) surface was cleaned by the well-established procedure[8] involving heat treatment in O_2 followed by a

vacuum anneal. The O_2 exposures were done in a background pressure of 2×10^{-6} Torr at 2000 K for 4 min with the sample heated from the back by electron bombardment. This procedure was usually done at the end of the day to allow the vacuum system to recover. Vacuum annealing consisted of *e*-beam heating the sample to 2300 K for 30 sec. Sample heating to temperatures less than 1600 K was accomplished by passing current through two 0.5-mm W rods approximately 10 mm in length, which were spot welded to the back of the crystal. Sample cleanliness was monitored by Auger electron spectroscopy.

Cu was evaporated onto the W(110) surface from high-purity Cu in a resistively heated, commercial W-wire basket. The Cu source was "broken in" by melting the Cu such as to wet the basket followed by an extensive bake at 1100 K. Following this procedure, no contaminants could be detected as a result of Cu deposition. The rate of deposition was controlled by varying the voltage across the basket and was monitored by a line-of-sight UTI 100C quadrupole mass spectrometer. The Cu coverages were established by temperature-programmed desorption (TPD).[9] All the data presented here involved films that were deposited at 90 K and annealed to 600 K.

ARUPS energy distributions were measured using a Vacuum Generators ADES-400 system with an unpolarized He-discharge lamp. The energy resolution of the electron analyzer was approximately 0.1 eV and the angular acceptance was about $\pm1°$. For most of the work reported here, the HeI photons ($h\nu=21.2$ eV) impinged on the sample surface at an incident angle of 10° and the photoelectrons were detected at various polar angles corresponding to $k_\parallel$ values along the $\bar{\Gamma}$-$\bar{H}$ symmetry line in the SBZ. The azimuthal detection angle to establish this SBZ symmetry orientation was established by low-energy electron diffraction (LEED).

B. Theoretical technique

The surface electronic-structure calculations utilized the LAPW method[10] modeling the 1 ML Cu/W(110) adsorption system as a five-layer W slab with pseudomorphic Cu adlayers on the exposed (110) surfaces. The W atoms of the slab were placed at bulk W positions. In the absence of actual structural measurements for the pseudomorphic Cu overlayer, total-energy calculations were performed for Cu atoms at long bridge, short bridge, and pseudothreefold adsorption sites as illustrated schematically in Fig. 1. The lowest energy corresponds to the long-bridge site, with the Cu nuclei at a height of 3.77 bohr above the outer layer of W nuclei. It is for this geometry that we report energy-level dispersions below. The calculations were semirelativistic,[10] and represented the effects of exchange and correlation with the local density-functional exchange-correlation potential[11] based on the Wigner interpolation formula.[12] Further details can be found in Ref. 13.

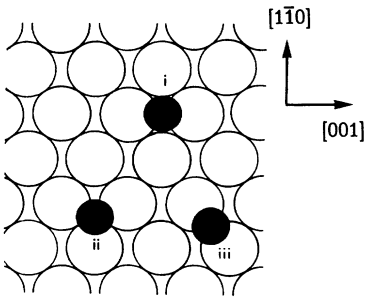

FIG. 1. A schematic representation of the (110) surface of a bcc lattice showing adsorbate atoms in the long-bridge or normal bcc site (i), one of the pseudo-threefold sites (ii), and in the short-bridge site (iii).

III. RESULTS

As has been discussed earlier,[6] an experimental fingerprint of electronic states that are localized at the interface is an ARUPS feature whose intensity rises monotonically with overlayer coverage up to 1 ML and then remains constant relative to substrate emission with further deposition. In order to select possible candidates, we begin by identifying Cu-derived features in the ARUPS energy-distribution curves (EDC's). Figure 2 shows a series of such curves taken at intervals along the $\bar{\Gamma}$-$\bar{H}$ symmetry line in the SBZ for both the clean and the 1 ML Cu/W(110) surfaces. These EDC's are given in terms of their $k_\parallel$ values relative to that corresponding to the zone boundary at $\bar{H}$, i.e., the value zero represents $k_\parallel$

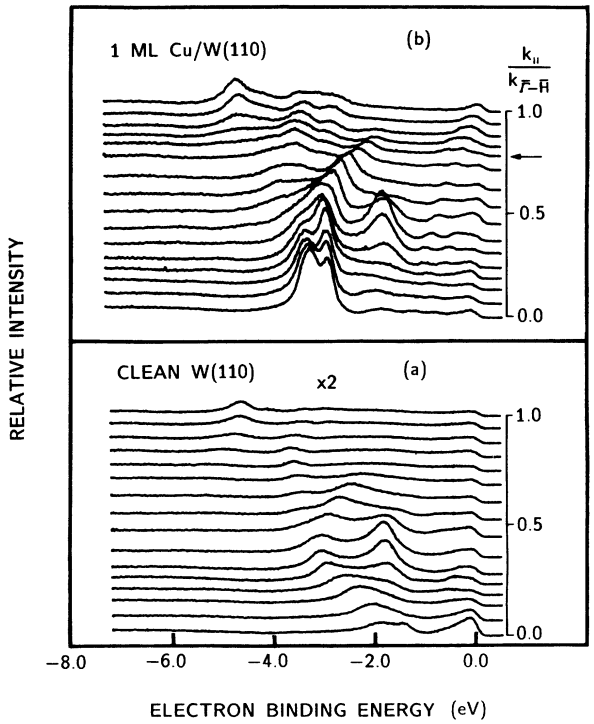

FIG. 2. He I ARUPS energy-distribution curves as a function of position in the SBZ along the $\bar{\Gamma}$-$\bar{H}$ symmetry line, where $k_\parallel/k_{\bar{\Gamma}\text{-}\bar{H}}$ refers to the ratio of the $k_\parallel$ value relative to its value at the $\bar{H}$ zone boundary, for a clean W(110) and (b) 1 ML Cu/W(110). The intensities for the clean W(110) results have been expanded by a factor of 2. The horizontal arrow (b) identifies the $0.82k_{\bar{\Gamma}\text{-}\bar{H}}$ data.

$=0$ or the $\bar{\Gamma}$ point, while 1.0 represents the $k_{\parallel}$ value at $\bar{H}$.

Figures 2(a) and 2(b) show that significant changes in the clean W spectrum results from the addition of the Cu. A major double-peaked feature can be seen near $k_{\parallel}=0$ centered at a binding energy near -3.0 ev. This structure rapidly decreases in intensity as the midzone is approached and appears to enhance the intensities of the dispersing clean-surface features seen beyond the midpoint. Dispersing structures at low binding energies can also be seen that appear to cross the Fermi energy near the $\bar{H}$ point. Further insight into the properties of these various states can be obtained by studying their behavior with respect to Cu coverage.

Figure 3 shows ARUPS EDC's corresponding to $k_{\parallel}=0.82k_{\bar{\Gamma}\text{-}\bar{H}}$, as function of Cu coverage. The same $k_{\parallel}$ for 1-ML coverage is indicated in Fig. 2(b) by an arrow. In order to make the interfacial nature of the various structures stand out, it is useful to normalize the EDC's relative to emission from the clean W surface. This can be done because Cu emission near the Fermi edge is negligible. Thus, the data presented in Fig. 3 are normalized to have the same Fermi-edge intensity.

From Fig. 3, the three main structures can be seen to grow monotonically above the W substrate contribution with Cu coverage. At this $k_{\parallel}$, the broad feature (possibly consisting of two separate peaks) just below the Fermi edge has an average binding energy (BE) of approximately -0.25 eV, a sharp intermediate peak appears at -2.12 eV, and the third broad feature lies near -3.5 eV. In going past the 1-ML Cu coverage (1.2 ML for the displaced curve of Fig. 3), another feature grows in at a BE of about -3.0 eV while the other structures slightly decrease in intensity. Throughout the growth of the second ML (not shown in Fig. 3), it is found that -0.25 and -2.12 eV features slowly diminish in intensity while the structure at -3.5 eV remains virtually constant in intensity. The structure at about -3.0 eV continues to strengthen. This overall behavior is strongly suggestive of the existence of interface states that can be verified by calculations on the clean and 1-ML Cu systems.

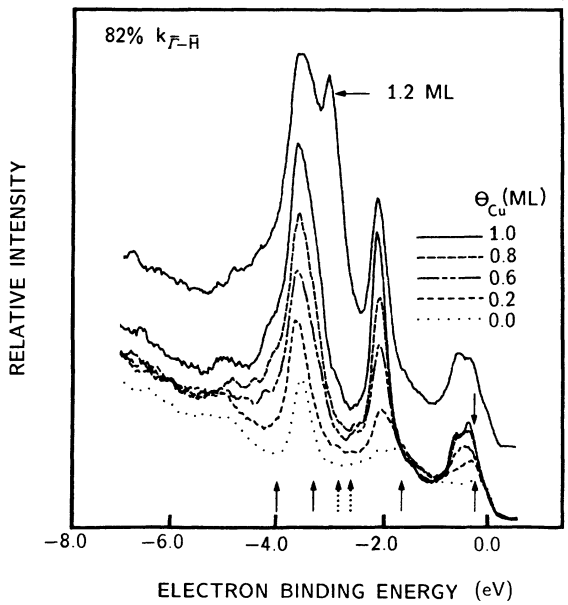

FIG. 3. He I ARUPS results at the $0.82k_{\bar{\Gamma}\text{-}\bar{H}}$ point in the SBZ as a function of Cu coverage. The displaced curve is for a Cu coverage of 1.2 ML and shows the appearance of a new feature for the Cu in excess of 1 ML marked by the horizontal arrow. The vertical solid arrows show the interface-state position and the dotted arrows the surface-state position predicted by the calculations.

In the calculations, we examine the wave functions, searching for those whose values are significant only in the outer two layers on either side of the seven-layer film. States which have appreciable values for both of the outer two layers (i.e., which are shared between the Cu's and the outermost W's) are referred to as interface states, while those which are appreciable only on the Cu overlayer itself are Cu surface states. As a criterion for singling out such states, we look for levels for which the probability of finding an electron in two outermost muffin tins on either side of the film relative to the sum over all muffin tins exceeds 80%. The set of states fitting this criterion near $0.82k_{\bar{\Gamma}\text{-}\bar{H}}$ is shown in Fig. 3 by the arrows with solid lines representing states with interface character and dotted ones showing those that are principally Cu surface states. As can be seen, the agreement is reasonably good except for the predicted levels at about -1.5 and -2.60 eV, which essentially bracket the observed peak near -2.12 eV.

A more complete description of the surface or interface states fitting our criterion at $0.83k_{\bar{\Gamma}\text{-}\bar{H}}$ is given in Table I. Here we list the binding energies, the relative surface or interface localization, and the relative symmetry character for each state. Each of the states listed in Table I appears in the calculation as a pair of levels split in BE by a few hundredths of an eV or less. This splitting is indicative of the magnitude of the interference effects resulting from the use of a slab model of only a few layers in thickness. In Table I, the values listed represent the average BE for these split states.

We can also follow the behavior of these various states along the $\bar{\Gamma}$-$\bar{H}$ symmetry line in the SBZ and compare with the experimental results. This comparison is shown in Fig. 4 for 13 points in the SBZ between $\bar{\Gamma}$ and $\bar{H}$. We note first from Table I that the calculations predict six closely spaced pairs of states at $0.83k_{\bar{\Gamma}\text{-}\bar{H}}$, which have the surface and interface character discussed above—these states are indicated by the solid circles on Fig. 4. The first state, which has interface character (i.e., is localized on the Cu and outermost W layers), has a binding energy of -0.18 eV at $0.83k_{\bar{\Gamma}\text{-}\bar{H}}$ and crosses the Fermi level close to the zone boundary. This state loses its localization near the zone center at a binding energy of approximately -0.7 eV. The symmetry of this state is predicted to be a mixture of $d\pi$ and $d\delta$. Another state is predicted at a binding energy of -1.57 eV at the $0.83k_{\bar{\Gamma}\text{-}\bar{H}}$ point with a principally $d\sigma$ symmetry. This state disperses to higher binding energies in going toward $\bar{\Gamma}$ and splits near $\bar{H}$. States having interface character are also predicted at binding energies near -3.1 and -4.05 eV dispersing to

TABLE I. $0.83k_{\bar{\Gamma}\text{-}\bar{H}}$.

Binding[a] energy (eV)	Surface or interface[b] character (%)			Cu-site symmetry[c] character (%)		
	Cu+W$^{(O)}$	Cu	W$^{(O)}$	$d\sigma$	$d\pi$	$d\delta$[d]
−0.18	99	40	60		58	42
−1.57	97	74	26	80	10	10
−2.61	94	93	7		30	70
−2.88	93	91	9		35	65
−3.10	81	65	35	36	64	
−4.05	88	58	42	17	65	18

[a]Binding energies are referenced to E_f and are rounded to three significant figures.
[b]Muffin-tin electron densities for both Cu and outer-W-layer muffin tins (W$^{(O)}$) have been normalized to the sum of contributions from all layer muffin tins.
[c]These numbers were obtained by integrating $|\psi_{lm}|^2$ in each muffin tin and expressing the result as a percentage of $\sum_{l,m}\int|\psi_{lm}|^2$ for all muffin tins.
[d]$d\sigma$ refers to orbitals with $d_{3z^2-r^2}$ symmetry characterization, while $d\pi$ refers to d_{xz} and d_{yz}, and $d\delta$ refers to d_{xy} and $d_{x^2-y^2}$.

lower binding toward the zone boundary. The first of these states also has mixed $d\pi$ and $d\delta$ symmetry, while the second has a significant additional $d\sigma$ component. In analogy with our findings for the 1ML Cu/Ru(0001) system, the interface states appear as two sets of bonding-antibonding pairs resulting from the strong Cu-W d-state hybridization. Finally, two states are predicted with binding energies centered at near −2.5 eV, which are highly localized on the Cu overlayer, i.e., Cu surface states. These states are predicted to disperse to lower binding energies near $\bar{H}$ and have mixed $d\pi$ and $d\delta$ symmetries.

The dispersion behavior of those experimental features, which have enough contrast to be definitively identified, is shown in Fig. 4 as solid lines. Here we see a reasonable agreement between calculations and experiment for both of the interface states, although the experiment indicates two states instead of one for the antibonding combination near the Fermi level. However, the agreement for the Cu surface states and the interface state at −1.57 eV is considerably less satisfying. Only one state can be clearly identified in this binding-energy region, and it disappears prior to reaching $\bar{H}$. In contrast, the calculations show the maximum degree of surface localization at the $\bar{H}$ point implying that these states should be seen with highest intensity at the zone boundary.

With respect to the possibility of an electronic effect in the adsorption of O on 1 ML Cu/W(110), we show in Fig. 5 ARUPS results for 1.1 ML Cu/W(110) as a function of O_2 exposure. The top curve is similar to that shown for a slightly higher coverage in Fig. 3, i.e., the shoulder near −3.0 eV is not as strong as for the 1.2-ML coverage case

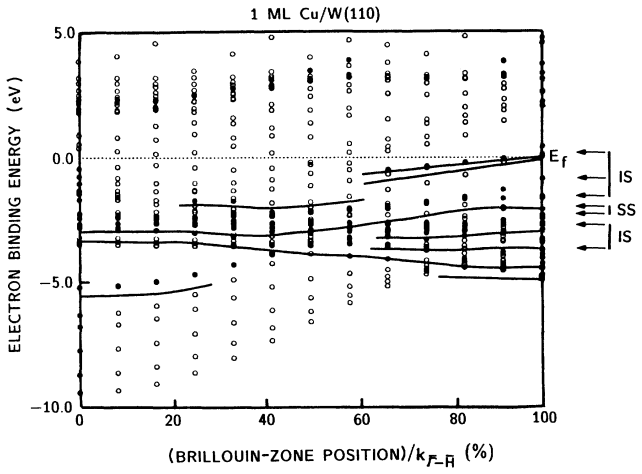

FIG. 4. A direct comparison of the calculated behavior of the surface and interface states along the $\bar{\Gamma}$-$\bar{H}$ line, measured as a percentage of the $k_{\parallel}$ value at the $\bar{H}$ zone boundary, for 1 ML Cu/W(110). Open circles indicate the positions of the various states making up the band structure, while the solid circles show those states which have relative surface or interface localizations greater than 80%. The horizontal arrows to the right give the surface or interface character of the predicted states.

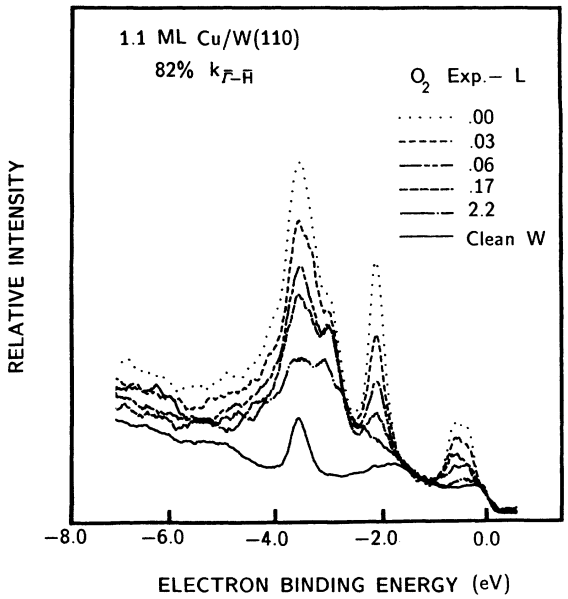

FIG. 5. The ARUPS results for (1.1 ML Cu)/W(110) taken at the $0.82k_{\bar{\Gamma}\text{-}\bar{H}}$ point as a function of O_2 exposure. The solid curve represents the clean W(110) result.

of Fig. 3. As this surface is exposed to O_2, several effects are evident in Fig. 5. There is a dramatic decrease in the intensity of all three of the major surface or interface structures and this "poisoning" is very sensitive to O coverage. It has been shown earlier that the initial sticking coefficient for O_2 on 1 ML Cu/W(110) is approximately one.[2] Therefore, the low-exposure values shown in the data of Fig. 5 directly translate into coverage, i.e., 0.06 ML O results in more than a 50% decrease in the intensity of all surface or interface features. Low-O_2 exposures simply reduce the intensity of the near-Fermi-edge structure, while the higher exposures appear to shift the feature to lower binding energies such that it crosses the Fermi level. A similar behavior can be seen for the feature near -3.5 eV but the shift is in the opposite difection. In contrast, the poisoning of the feature near -2.0 eV is complete for the 2.2-L exposure (1 langmuir $=1\times10^{-6}$ Torr sec) with no appreciable shift in peak position. In addition, we see that the shoulder near -3.0 eV identified with the Cu in the second layer is not appreciably affected by O adsorption.

Finally in Fig. 6, we show the effect of O adsorption on the LEED pattern for two of the exposures of Fig. 5. Figure 6(a) shows the results for the clean 1.0 ML Cu/W(110) surface. Except for an increase in the brightness of the spots, the pattern is identical to that seen for the clean W(110) surface, indicating that the overlayer growth is pseudomorphic.[14] An O_2 exposure of 0.06 L results in the LEED pattern of Fig. 6(b), which indicates a slight increase in the background intensity and the appearance of outboard-satellite spots in the $[1\bar{1}0]$ direction. Figure 6(c) shows the results of a 2.2-L O_2 exposure and is characterized by a slightly broadened and considerably weaker set of (1×1) and satellite spots and a significantly increased intensity in the background.

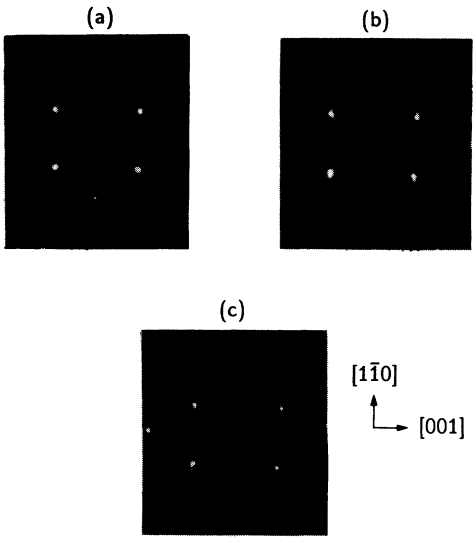

FIG. 6. LEED results for O_2 interacting with 1 ML Cu/W(110). (a) a (1×1) LEED pattern identical with that from clean W(110) (except more intense); (b) the effect of a 0.06-L O_2 exposure, (c) the patterns for a 2.2-L O_2 exposure.

IV. DISCUSSION

In investigating the electronic properties of the Cu/W(110) bimetallic system, we find behavior very similar to that first characterized for Cu/Ru(0001),[6] although the agreement between experiment and the calculations illustrated in Fig. 4 is not as good as that found for either the Cu/Ru(0001) or the Ni/Ru(0001) systems.[7] The overall agreement for the dispersion behavior is seen to be good in Fig. 4, but significant discrepancies in the binding-energy values are evident. Our present calculations predict the existence of two Cu surface states and four interface states at the $0.83k_{\bar{\Gamma}\text{-}\bar{H}}$ point, while the experimental results show evidence for only one surface state and the antibonding component of the interface states appears as a doublet. In addition, the experimental results show the intensity of the Cu surface state decreasing near the $\bar{H}$ point, while the calculations indicate good localization at that point. This discrepancy must be due to a photoemission transition matrix element effect rather than a discrepancy in the predicted degree of localization. The binding-energy values are in good agreement for the interface-state feature near the Fermi level, but discrepancies of several tenths of an eV are seen for all other features. This lack of detailed agreement is not surprising, considering that our LAPW calculations do not include spin-orbit coupling. For example, relativistic effects account for level splittings of 0.5 to 1.0 eV in the electronic structure W(001).[15]

We have no explanation for the results reported recently by Lilienkamp, Koziol, and Bauer,[16] in which no evidence was found for Cu/W(110) interface states. These authors performed ARUPS principally along the $\bar{\Gamma}$-$\bar{H}$ and $\bar{\Gamma}$-$\bar{M}$ symmetry lines and found "nothing comparable (to the interface states reported in Ref. 6) at any thickness, emission azimuth and angle." It is difficult to comment on this statement since the only coverage-dependence data presented in Ref. 16 are for normal emission where surface and interface-state behavior tend to have the least contrast. However, even at this point in the SBZ, we find the fingerprint of Cu/W(110) interface states when we exercise sufficient care.

Qualitatively, the conclusions drawn from the experimental-theoretical comparison of Fig. 4 are similar to those reached for the Cu/Ru(0001) system.[6] There are three sets of states resulting from Cu adsorption. There are virtually pure Cu surface states, and there are bonding and antibonding Cu-W interface states whose splitting is a measure of the degree of Cu $3d$ – W $4d$ hybridization. In principle, this splitting would include contributions from both the hybridization interaction and the energy offset between the Cu $3d$ band and the W $4d$ one. However, the W d bands split into an occupied manifold whose centroid is close to that of the Cu $3d$ band, and an unoccupied manifold well above the Fermi level (E_f for W lies in a valley in the density of states, as is characteristic of bcc crystals). Ignoring hybridization involving the unoccupied manifold of W $4d$, the offset between the interacting Cu and W d bands is small. Correspondingly, the interface-state wave functions are evenly shared by Cu and outer-layer W atoms, and the splitting of the

bonding and antibonding levels can be attributed essentially entirely to Cu-W hybridization. This is similar to the situation for Cu/Ru, for which the Cu $3d$–Ru $4d$ band offset near the zone edge is also small, and less similar to the Ni/Ru case where the overlayer $3d$ bands lie higher.

Near the point $\bar{H}$ in the SBZ, Fig. 3 indicates that the bonding-antibonding splitting of the Cu-W interface states is roughly 3.0 eV. For Cu/Ru(0001), the splitting was 2.2 eV. Although some of this difference is due to the fact that the Cu-W interface states are not quite as "interfacial" (i.e., evenly shared between the Cu and outermost W layers) as for Cu/Ru (Table I),[6,17] the net result is that the feature corresponding to the antibonding combination of interface states is closer to the Fermi energy for Cu/W (~ -0.5 eV) than for Cu/Ru (~ -1.5 eV) at this point in the SBZ. States near the Fermi level have more of a "frontier" character,[18] and this, coupled with their partial π symmetry, is what prompted our investigating the possibility of a chemical involvement of the interface states.

In the W band structure there is a band gap that opens up near the zone boundary along the symmetry line $\bar{\Gamma}$-$\bar{H}$. A similar gap is seen for Ru[7] and Cu[19] near $\bar{K}$. From Fig. 4, we see that this gap for W is approximately 4 eV while the calculated gaps for Ru and Cu are found to be about 2.3 (Ref. 7) and 1.6 (Ref. 19), respectively. The Cu-substrate hybridization interaction is seen in Fig. 4 to open up a similar gap in the bimetallic overlayer systems near the zone boundary. However because this interaction is smaller than for the substrate-substrate interaction, the gap is narrower, which pulls the states out of the bulk bands and isolates them as impuritylike states on the outermost layers (i.e., interface states). As one moves along the $\bar{\Gamma}$-$\bar{H}$ line toward $\bar{\Gamma}$, the gap narrows and the surface or interface states become members of the bulk bands (near the $0.60k_{\bar{\Gamma}-\bar{H}}$ point in Fig. 4) losing their surface or interface localization and disappearing from the photoemission spectra.

The zone-boundary gaps for bulk Cu, Ru, and W (1.6, 2.2, and 3.0 eV, respectively) scale approximately as the d-band widths in these transition metals (3.0, 6.0, and 9.0 eV, respectively).[19] Again, the bonding-antibonding splitting of the interface states, which is a measure of the strength of the Cu-substrate hybridization interaction, scales as 1.6, 2.2, and 3.0 eV for Cu/Cu, Cu/Ru, and Cu/W, respectively.

With respect to the chemical nature of the Cu/W surface, we see that, as a result of the strong Cu/W hybridization, the electronic properties of the Cu overlayer take on a more W-like appearance. Indeed, the local Cu d density of states has a small component that resides above the Fermi level, which means that this layer is no longer entirely noble in character. From an electronic standpoint, Cu has taken on an appearance more like that of Ni. These are, of course, greatly oversimplified characterizations. However, it seems reasonable to expect that the Cu overlayer on W(110) would have an altered chemical behavior as compared to bulk Cu.

Characterizing the effect of Cu's altered electronic makeup on surface chemical behavior is difficult because of the presence of the more active W substrate. This effect is dramatically illustrated by the O/Cu/W(110) work reported earlier by Gomer and coworkers.[2] As mentioned before, 1 ML of Cu facilitates the dissociative sticking of O_2 on the bimetallic surface, increasing the sticking coefficient to a value near 1 from about 0.5 for clean W(110) and increasing the saturation O coverage from about $\frac{2}{3}$ to more than $\frac{3}{4}$ ML. However, O chemisorbed on overlayer Cu is a metastable situation since the competition for the oxygen is strongly weighted toward W. At temperatures just above 300 K this metastability manifests itself as a segregation of the Cu into 3D islands interspersed with islands of chemisorbed O having local O coverages near one,[2] a coverage which is impossible to achieve simply by O_2 exposures. This tendency for Cu-atom displacement with O chemisorption is evident even at low temperatures in the LEED results of Fig. 6(b).

The appearance of outboard satellites in the pattern of low-coverage O chemisorbed on 1 ML Cu/W(110) is consistent with the O producing a modulation in the Cu overlayer lattice spacing along the $[1\bar{1}0]$ direction with a superperiod of approximately 15 lattice spacings. The displacements would be such as to result in a $[1\bar{1}0]$ lattice spacing, which, on the average, is smaller than for the pseudomorphic case. These regions are then separated by misfit dislocations as seen, for example, for 2 ML of Cu on the Ru(0001) surface.[20] A similar situation is also seen during growth of the second ML of Cu on the W(110) surface where the Cu-Cu interaction is no longer able to support the large interfacial strain caused by the natural misfit between the W(110) pseudomorphic sites and those of the closest-matched Cu(111) lattice. In both cases, the situation is similar to that discussed by Novaco and McTague[21] for the periodic strains seen at strained heterogeneous interfaces.

The fact that the periodic strains suggested by the LEED pattern of Fig. 6(b), and shown schematically in Fig. 7, are perpendicular to the direction of maximum misfit strain—a pseudomorphic Cu(111) lattice is strained by only about 2% in the $[1\bar{1}0]$ direction and by almost 25% in the [001] direction on the W(110) surface—leads one to suspect that the Cu atoms move more easily along the $[1\bar{1}0]$ direction than along [001]. In order to investigate this idea, we carried out total-energy calculations corresponding to placement of the

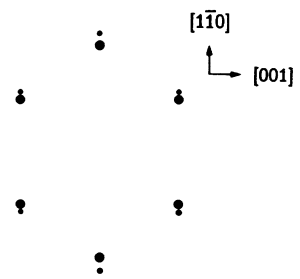

FIG. 7. A schematic LEED pattern corresponding to the data of Fig. 5(b). The outboard satellites indicate a superlattice period of approximately 15 in the $[1\bar{1}0]$ direction.

pseudomorphic Cu overlayer lattice at various sites on the W(110) surface. Figure 1 illustrates Cu adatoms at the long-bridge site (i), (the normal next-layer bcc site) on this surface, at one of the pseudothreefold sites (ii), and at the short-bridge site (iii). The calculations indicate that bonding at the first two of these sites is favored by roughly 0.7 eV relative to the short bridge, while the long bridge is favored over the pseudothreefold site by only about 50 meV. Thus, the Cu adatoms are relatively free to move along the $[1\bar{1}0]$ direction between the long bridge and pseudothreefold sites, which implies that the phonon properties for the Cu/W(110) bimetallic system should be highly anisotropic.

The situation becomes less well defined for higher O coverages. Figure 6(c) shows the LEED pattern resulting from a 2.2 L O_2 exposure at 90 K. Under this condition, the (1×1) and satellite spots have been broadened, and there has been a considerable increase in the intensity of the diffuse background. Clearly, high-coverage O causes virtually a random disordering of the overlayer, and we suggest that it is this disordering effect that is largely responsible for the poisoning of the surface and interface-state intensities with O coverage that is illustrated in Fig. 5.

Using the above conclusions to make a statement on the origin of the increase in dissociative sticking coefficient for O_2 on the 1 ML Cu/W(110) surface is a risky exercise. Our experiments involving O adsorption only probe the system in its steady-state configuration and, because the structures are unknown, calculations are not presently possible even in this state. Dissociative sticking is a multistep process of considerable complexity that includes at least the accommodation into one or more mobile precursor states—the search over the surface for an "active" dissociation site and the dissociation at this site into two chemisorbed O atoms. At this point, it is not at all clear just which of these is rate limiting for the overall process.

Lin, Shamir, and Gomer[3] suggest that the rate-limiting step for O adsorption is the initial accommodation into the mobile precursor state and that increased dissociative sticking for the 1 ML Cu/W(110) is a consequence of the existence of soft translational phonon modes for this case. These authors state that there is some support for this contention in that the LEED pattern for saturation O_2 exposures is dramatically disturbed for the 1-ML case, while little effect is seen for 2 ML. We have confirmed the LEED results and show that the chemisorbed O on the 1 ML Cu/W(110) causes some surface rearrangement as evidenced by the appearance of outboard satellites along the $[1\bar{1}0]$ direction. Our calculations show that Cu displacement along this direction requires little energy. We now discuss in a bit more detail the possible consequences of this behavior on O_2 dissociative sticking.

As we mentioned above, dissociative sticking occurs in at least two steps: first, initial accommodation into the mobile precursor state and second, the dissocation into chemisorbed O atoms. With respect to accommodation, there are two important factors involved: (1) the mass of the incoming molecule relative to the "effective" mass of the surface atoms involved in the energy-loss process and (2) the attractive interaction potential between the surface and molecular species. According to the hard-cube model of gas-surface interactions,[22] for a low-temperature surface and for molecules approaching the surface at normal incidence, accommodation will occur when the well depth U of the interaction potential is greater than the mean translational energy of the incident gas molecule u_0 times the quantity $(\mu-1)^2/4\mu$, where μ is the ratio of the molecular mass to the "effective" mass of the surface interaction.

The effective mass for the collision is determined by the average range over which substrate atoms collectively cooperate in the collisional-loss process. This range can be approximated by the product of the velocity of sound in the substrate material and the average time over which the repulsive interaction takes place.[22] It is this aspect of the accommodation process that is related to the phonon character of the substrate material. Everything else being equal, the "softer" the phonon spectrum the smaller the velocity of sound and the closer the effective mass value is to the mass of a surface atom, i.e., the interaction looks more like a binary collision.[22]

In analyzing the collisional behavior of Ar scattered off a W surface (which is reasonably close to O_2/W) an effective mass value of 760 amu was obtained.[22] Thus from the relationship above, accommodation would require an attractive potential-well depth greater than approximately five times the incident molecular kinetic energy (again, assuming normal incidence). In contrast, assuming the same phonon properties, a Cu overlayer would require a well depth of only about 1.5 times the incident energy. If the phonon spectrum for the Cu overlayer is softer than for W, this well-depth requirement would be diminished further. From this crude analysis, it seems clear that regardless of the details of the phonon properties the Cu overlayer will act as a good impedance-matching layer and increase the initial accommodation of O_2 into the precursor state.

The second aspect of dissocative sticking is, of course, the availability of sites which are reactive to the dissociation process. We have seen how the inclusion of a Cu overlayer can increase the accommodation, and this process can be anticipated to be about as effective for the second Cu ML as the first. The second ML is found to have an initial dissociative sticking coefficient of about 0.5. However, this value is only maintained to an O coverage of about 5%, above which the value rapidly decreases approaching that for bulk Cu for O coverages above about 15%.[2] This behavior is probably more the result of the presence of a small number of defects in the 2-ML Cu film rather than its unique chemical character. It seems clear then that the 1-ML case has a unique enhancement in reactivity for O_2 dissocation from the precursor state. This conclusion, along with our LEED results and binding-site calculations, leads us to believe that the origin of the 1-ML reactivity is the ability of Cu atoms to displace in the presence of an O_2 molecule and increase the molecule's access to the active substrate.

The effect is illustrated in Fig. 8. Here we see that moving neighboring Cu atoms to opposite pseudothreefold sites opens enough space for an O_2 molecule to

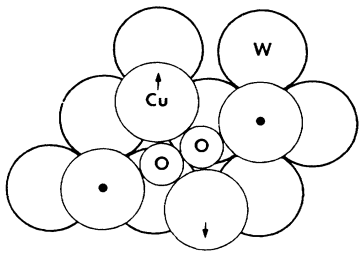

FIG. 8. A schematic representation of the fact that an O_2 molecule can access the underlying W(110) surface if neighboring Cu atoms are moved into pseudo-threefold adsorption sites. The W and Cu atomic radii correspond to their values for bulk solids, i.e., 1.34 and 1.28 Å, respectively, and the individual O_2 atom radii are set to be as large as possible in order to contact the displaced Cu. This procedure results in O radii of 0.67 Å.

nestle between Cu atoms and gain access to the underlying W surface. The O_2 atomic radii in this figure have been chosen to bring them in contact with the neighboring Cu atoms, which results in a value for the radius of 0.67 Å. This compares with a tabulated value of 0.62 Å for the doubly bonded oxygen molecule.[23] Thus, it seems plausible that the O_2 molecule could have an increased W interaction as a result of the ability of surface Cu atoms to move along the $[1\bar{1}0]$ direction.

The effects that we have just described depend both on the fact that Cu is a smaller atom than W (giving it space to move in a pseudomorphic structure) and on the fact that Cu is basically a spherical atom. This means that Cu does not have the same directional-bonding character as, for example, W that would lock it into the bcc or long-bridge surface site. This idea suggests an initial test of our conclusions.

Re is the nearest neighbor to W on the right side of the periodic table and is the first hcp-structured element on this side of the $5d$ series. The overall O_2 adsorption chemistry of the Re(0001) surface should be similar to that of W(110), i.e., reasonable precursor accommodation and active dissociation kinetics, and we can anticipate that 1 ML Cu would again promote precursor accommodation. However, the close-packed Re(0001) surface should inhibit Cu displacement and suppress the enhanced dissociative sticking coefficient. Measurements of sticking of O_2 on Cu/Re(0001) should permit one to delineate between an electronic effect, possibly due to the intervention of surface and interface states, and effects which result from unique overlayer mechanical or structural properties. Of course, these electronic states will be different than those found for the Cu/W system. The authors are aware of no sticking coefficient measurements for O_2/Cu/Re(0001) in the literature.

V. CONCLUSIONS

The present studies of the electronic and structural properties of the 1 ML Cu/W(110) bimetallic surface and their behavior with respect to O chemisorption permit the following conclusions to be drawn:

(1) Cu is confirmed to grow during the first ML in a pseudomorphic structure with respect to the W(110) surface.[14]

(2) Photoemission results, along with theoretical calculations, indicate that the 1 ML Cu/W(110) surface is electronically characterized by a set of surface and interface states resulting from the strong Cu $3d$–W $5d$ hybridization interaction; the interaction strength being intermediate between that due to W-W and Cu-Cu. The antibonding component of the bonding interaction results in states which are shared between the Cu overlayer and the first W layer and a small portion of these states appear above the Fermi level near the zone boundary at $\bar{H}$. Thus, qualitatively, the Cu layer is not noble like bulk Cu but has properties more like those of a bulk Ni surface.

(3) The discrepancies that are seen in the comparison of the experimental and theoretical results are attributed to neglect of relativistic effects in our calculations for W, which is known to give rise to significant errors.[15]

(4) Chemisorbed O rapidly poisons all of the surface and interface states. The Cu surface state completely disappears from the photoemission spectrum (at the $0.82k_{\bar{\Gamma}\text{-}\bar{H}}$ point in the SBZ) after an O_2 exposure of 2.2 L (a coverage of about 0.67 ML). The interface states are not completely eliminated by this O_2 exposure, and the bonding-antibonding splitting increases at the higher coverages.

(5) According to LEED, low coverages of O result in outboard satellites along the $[1\bar{1}0]$ direction with a superperiod of about 15 lattice constants along the low-strain $[1\bar{1}0]$ direction. This structure is consistent with the existence of Cu islands of modulated strain having an average lattice constant smaller than that for W(110) separated by misfit dislocations having an average separation of ~ 15 lattice constants.[20] Higher coverages result in a broadening of both the (1×1) and satellite spots, a decrease in their (1×1) intensities and an increase in the diffuse background.

(6) We believe that these structural changes with O coverage are responsible for the poisoning of the surface and interface states. From the behavior of the Cu surface state with O coverage, we further suggest that the high-coverage Cu overlayer has, on the average, a (1×1) structure but that the relative separation of neighboring sites is random over a spatial region around the average lattice site. The spatial extent of this region depends sensitively on the O coverage.

(7) We suggest further that the unique increase in the O_2 dissociative sticking coefficient observed for the 1 ML Cu/W(110) system[3] results from the increased energy transfer from O_2 to the light Cu coupled with the ability of the Cu atoms to displace easily along the $[1\bar{1}0]$ direction, which allows O_2 continued access to the more active W surface.

ACKNOWLEDGMENTS

The authors would like to express their appreciation to Professor R. Gomer for motivating this work and for many stimulating discussions concerning the results. The portion of the work done at Sandia National Laboratory was supported in part by the U.S. Department of Energy, Office of Basic Energy Sciences, Division of Materials Sciences, under Contract No. DE-AC04-76DP00789.

*Present address: Technology Development Laboratory, Corporate Research/3M, St. Paul, MN 55144.

[1]D. W. Goodman and J. E. Houston, Science **236**, 403 (1987).
[2]J. C. Lin, N. Shamir, and R. Gomer, Surf. Sci. **206**, 61 (1988).
[3]J. C. Lin, N. Shamir, and R. Gomer, Surf. Sci. **206**, 86 (1988).
[4]N. Shamir, J. C. Lin, and R. Gomer, J. Chem. Phys. **90**, 5135 (1989).
[5]F. H. P. M. Habraken, E. P. Kieffer, and G. A. Boatsma, Surf. Sci. **83**, 45 (1979).
[6]J. E. Houston, C. H. F. Peden, P. J. Feibelman, and D. R. Hamann, Phys. Rev. Lett. **56**, 375 (1986).
[7]J. E. Houston, J. M. White, P. J. Feibelman, and D. R. Hamann, Phys. Rev. B **38**, 12 164 (1988).
[8]See, for example, J. E. Houston and T. E. Madey, Phys. Rev. B **26**, 554 (1982).
[9]P. J. Berlowitz, J. E. Houston, J. M. White, and D. W. Goodman, Surf. Sci. **205**, 1 (1988).
[10]D. R. Hamann, L. Mattheiss, and H. S. Greenside, Phys. Rev. B **24**, 6151 (1981).
[11]*Theory of the Inhomogeneous Electron Gas,* edited by S. Lundquist and N. H. March (Plenum, New York, 1983).
[12]E. Wigner, Phys. Rev. **46**, 1002 (1934).
[13]L. Mattheiss and D. R. Hamann, Phys. Rev. B **33**, 823 (1986).
[14]E. Bauer, H. Poppa, G. Todd, and F. Bonczek, J. Appl. Phys. **45**, 5164 (1974); E. Bauer and H. Poppa, Thin Solid Films **121**, 159 (1984); M. Tikhov, M. Stolzenberg, and E. Bauer, Phys. Rev. B **36**, 8719 (1987); see also N. J. Taylor, Surf. Sci. **4**, 161 (1966).
[15]L. Mattheiss and D. R. Hamann, Phys. Rev. B **29**, 5372 (1984).
[16]G. Lilienkamp, C. Koziol, and E. Bauer, Surf. Sci. **226**, 358 (1990).
[17]J. E. Houston, C. H. F. Peden, P. J. Feibelman, and D. R. Hamann, Surf. Sci. **192**, 457 (1987).
[18]R. Hoffman, *Solids and Surfaces: A Chemist's View of Bonding in Extended Structures* (VCH, New York, 1988).
[19]D. A. Papaconstantopoulas, *Handbook of the Band Structures of Elemental Solids* (Plenum, New York, 1986).
[20]G. O. Pötschke and R. J. Behm, Phys. Rev. B **44**, 1442 (1991).
[21]A. D. Novaco and J. P. McTague, Phys. Rev. Lett. **38**, 1286 (1977).
[22]E. K. Grimmelmann, J. C. Tully, and M. J. Cardillo, J. Chem. Phys. **72**, 1039 (1980).
[23]L. Pauling, *The Nature of the Chemical Bond,* 3rd ed. (Cornell University Press, Ithaca, NY, 1959), p. 228.

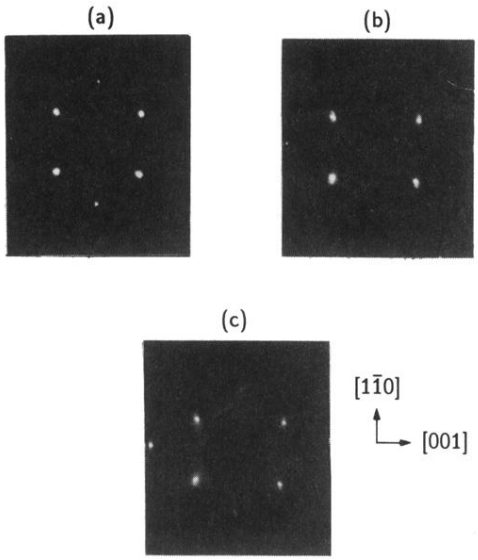

FIG. 6. LEED results for O_2 interacting with 1 ML Cu/W(110). (a) a (1×1) LEED pattern identical with that from clean W(110) (except more intense); (b) the effect of a 0.06-L O_2 exposure, (c) the patterns for a 2.2-L O_2 exposure.